

Probing Covalency in the UO_3 Polymorphs by U M_4 edge HR-XANES

Y Podkovyrina¹, I Pidchenko², T Prüßmann², S Bahl², J. Göttlicher³, A Soldatov¹, T Vitova²

¹International Research Center “Smart Materials”, Southern Federal University, ul. Zorge 5, 344090 Rostov-on-Don, Russia

²Karlsruhe Institute of Technology, Institute for Nuclear Waste Disposal, P.O. Box 3640, D-76021 Karlsruhe, Germany

³Karlsruhe Institute of Technology, ANKA Synchrotron Radiation Facility, P.O. Box 3640, D-76021 Karlsruhe, Germany

E-mail: podkovyrina@sfedu.ru

Abstract. Local atomic and electronic structure investigations of uranium trioxide (UO_3) crystalline phases performed by the U M_4 edge HR-XANES technique is presented. The experimental U M_4 edge HR-XANES spectra of α - UO_3 , β - UO_3 and γ - UO_3 polymorphic phases are compared with spectra of uranate (CaU_2O_7) and uranyl ($\text{UO}_3 \cdot 1-2(\text{H}_2\text{O})$) compounds. We describe a finger print approach valuable for characterization of variations of U-O axial bond lengths. Theoretical calculations of spectra using full-multiple-scattering theory (FEFF9.6 code) are performed. We have tested and selected input parameters, which provide best agreement between experimental and calculated spectra.

1. Introduction

Both structural and electronic properties of the uranium oxides are of fundamental and practical interest primarily due to the role of UO_2 in the nuclear fuel cycle [1, 2]. UO_2 is commonly exposed to oxidizing conditions and other binary oxides like for example UO_3 and U_3O_8 form at different stages of the nuclear fuel cycle [3]. UO_3 has the highest oxygen content among the uranium oxides. The chemical and physical properties of its polymorphs are also important to mining, milling, refinement and conversion processes that precede isotope enrichment within a nuclear fuel cycle [4]. X-ray absorption fine structure (XAFS) spectroscopy is successfully used for electronic and geometric structural investigations of uranium bearing materials [5]. The high energy resolution XAFS technique has gained popularity in the last years for structural investigations of broad range of materials [6]. The high energy resolution X-ray absorption near edge structure (HR-XANES) spectra at the U M_4 edge ($3d_{3/2} \rightarrow 5f$) have spectral features with reduced broadening compared to the conventionally measured XANES [7-9]. Therefore this advanced technique provides relative energy positions of valence unoccupied actinide (An) f orbitals not accessible by the conventional XANES method [7-9]. In this study we discuss a finger print approach for detection of changes in the bond lengths between U and the two axial O atoms in uranyl type of bonding, i.e. U(VI) forms short ($< 1.8 \text{ \AA}$) covalent axial bonding with two O atoms (U-O_{ax}). We present results of theoretical «*ab-initio*» full-multiple-scattering (FMS) HR-XANES calculations for the α - UO_3 , β - UO_3 and γ - UO_3 phases by the FEFF 9.6 code [10].



2. Experiments and calculations

The α - UO_3 and β - UO_3 phases were synthesized as reported in [3]; γ - UO_3 is a commercial sample (Cameco Corp.); metaschoepite is prepared as reported in [11]. CaU_2O_7 was synthesized by recrystallizing $\text{UO}_3 \cdot 1-2(\text{H}_2\text{O})$ in concentrated CaCl_2 aqueous solution. The structures of the studied compounds were confirmed by powder XRD measurements performed at the SUL-X beamline at ANKA (estimated purity > 95%). The obtained XRD patterns were compared with patterns from the PDF database (ICDD, [12]) using the DIFFRAC.EVA, Bruker software. Each compound with about 10 wt % of U was mixed with cellulose powder and pressed into a pellet. The U M_4 edge HR-XANES spectra of $\text{UO}_3 \cdot 1-2(\text{H}_2\text{O})$, CaU_2O_7 , α - UO_3 , β - UO_3 and γ - UO_3 were measured using Johann type X-ray emission spectrometer recently installed at the INE-Beamline for actinide research at the ANKA synchrotron radiation facility, Karlsruhe; Germany [13,14]. The incident energy was monochromatized by a Si(111) double crystal monochromator (DCM). The sample, analyzer crystals and a silicon drift detector (KETEK) were arranged in a vertical Rowland geometry. The U HR-XANES spectra at the M_4 -edge were obtained by recording the maximum intensity of the M_β emission line (U M_β 3337 eV) with five spherically bent Si(220) crystal analyzers with 1 m bending radius. The crystals were aligned at 75° Bragg angle. The DCM was calibrated by assigning 3725.5 eV to the maximum of the WL of a U M_4 edge HR-XANES spectrum of a UO_2 sample, which was repeatedly measured during the experiments.

The U M_4 HR-XANES spectra were calculated with the FEFF9.6 «*ab-initio*» quantum chemical code based on the full-multiple-scattering theory (FMS). The algorithm for the FMS method has been described elsewhere [15]. Phase shifts of the photoelectron were calculated in the framework of the self-consistent crystal muffin-tin (MT) potential scheme with 15% overlapping MT spheres. The spectra have been simulated using several types of exchange potentials: non-local, Dirac-Fock, Hedin-Lundquist or Dirac-Hara potentials. The best agreement with experiment has been achieved for the spectra calculated with the Hedin-Lundquist potential in Final State Rule (FSR) approximation for core-hole, reducing the $3d_{3/2}$ core-hole life-time broadening (3.5 eV) to 2 eV and correcting the Fermi energy for $\text{UO}_3 \cdot 1-2(\text{H}_2\text{O})$ and CaU_2O_7 by 0.5 eV. The atomic potentials were calculated self consistently for cluster sizes of about 7.0 Å around the absorber (including 101 atoms), while FMS calculations of U M_4 HR-XANES were performed for cluster of 10 Å radii (285 atoms). For the simulations of the HR-XANES spectra we have used the crystallographic data presented in Table 1.

Table 1. Crystallographic data used for calculations of the U M_4 HR-XANES spectra.

| Phase | Space group | Crystal system | Lattice parameters | #ICSD |
|---|----------------|----------------|---|--------|
| α - UO_3 | P-3m1 (#164) | Trigonal | $a=b=3.97$ $c=4.16$ $\alpha=\beta=90^\circ$ $\gamma=120^\circ$ | 31628 |
| β - UO_3 | P121 1 (#4) | Monoclinic | $a=3.91$ $b=14.33$ $c=10.34$ $\alpha=\beta=\gamma=90^\circ$ | 14314 |
| γ - UO_3 | I41/amd (#141) | Tetragonal | $a=b=6.90$ $c=19.97$ $\alpha=\beta=\gamma=90^\circ$ | 1093 |
| $\text{UO}_3 \cdot 1-2(\text{H}_2\text{O})$ | Pbcn (#60) | Orthorhombic | $a=14.68$ $b=14.02$ $c=16.71$ $\alpha=\beta=\gamma=90^\circ$ | 31631 |
| CaU_2O_7 | R-3m (#166) | Trigonal | $a=b=c=6.26$ $\alpha=36.32$, $\beta=\gamma=90^\circ$ | 156714 |

3. Results and discussion

The U M_4 HR-XANES spectra of UO_3 polymorphs are compared with the spectra of $\text{UO}_3 \cdot 1-2(\text{H}_2\text{O})$ and CaU_2O_7 (fig. 1a). All U M_4 HR-XANES spectra have three distinct spectral features marked with A (~ 3727 eV), B (~ 3729 eV) and C (~ 3732 eV) in figure 1a. The A, B and C peaks have been assigned to electronic transitions of $3d_{3/2}$ electrons to $5f\delta/5f\phi$ (A), $5f\pi$ (B) and $5f\sigma$ (C) unoccupied valence orbitals of U(VI) in the form of UO_2^{2+} (uranyl) [8]. The hybridized U 5f and 6p orbitals form sigma

covalent bonds mainly with 2p orbitals of the Oax atoms therefore the energy position of peak C is essentially influenced by variations of the U-Oax bond length [9].

U forms uranyl and long > 1.8 Å (uranate) U-Oax bonds in metaschoepite (1.78 Å) and CaU_2O_7 (1.94 Å), respectively. These differences in bond lengths are reflected by the energy positions of peaks A, B and C. Peak A is shifted to higher energies (+ 0.2 eV), whereas peaks B (- 0.2 eV) and particularly C (- 1.1 eV) are shifted to lower energies for CaU_2O_7 compared to metaschoepite ($\text{UO}_3 \cdot 1-2(\text{H}_2\text{O})$). The elongation of the U-Oax in CaU_2O_7 leads to less electronic density in the vicinity of U, i.e. increased ionicity of the U-Oax bond [16]; as a result, due to worse screening of the core-hole, the main peak A is shifted to higher energies compare to this peak for the metaschoepite spectrum. The energy position of peak B can be in principle influenced by variations of the U-Oax but also by changes in bonding distances between U and the equatorial ligands.

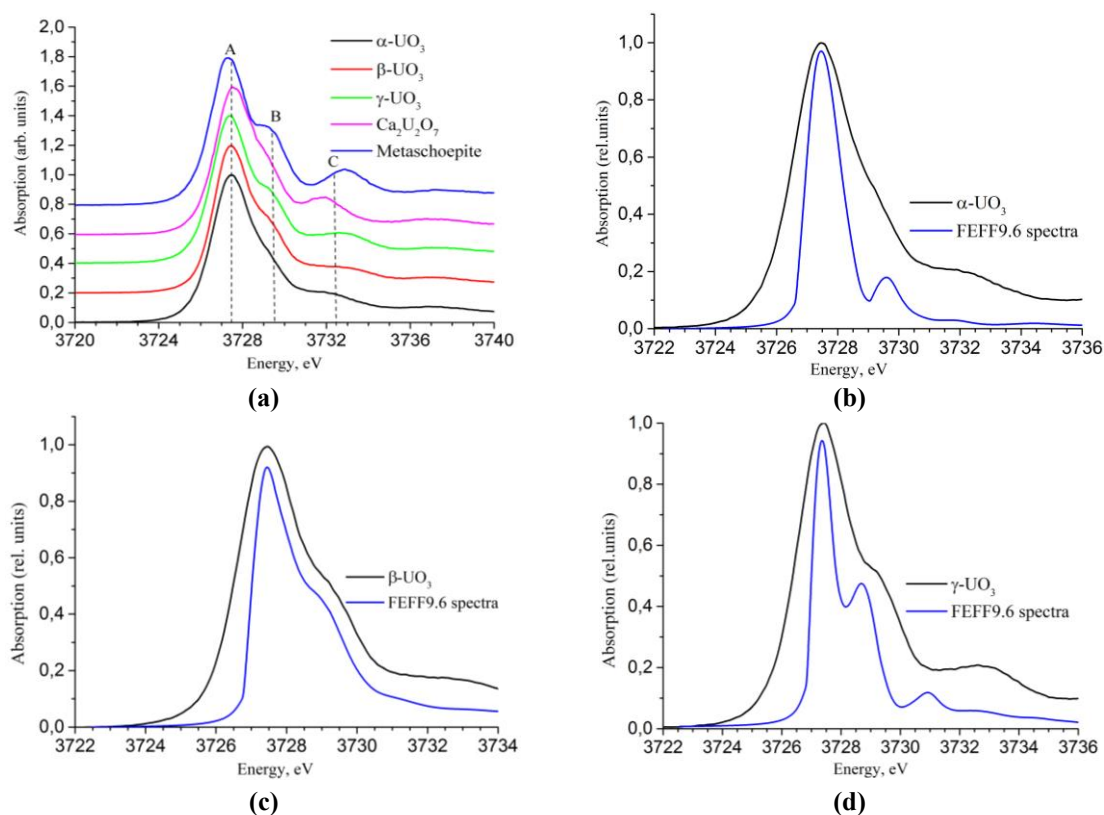


Figure 1. U M_4 HR-XANES spectra of $\text{UO}_3 \cdot 1-2(\text{H}_2\text{O})$, CaU_2O_7 , $\alpha\text{-UO}_3$, $\beta\text{-UO}_3$ and $\gamma\text{-UO}_3$ (a), experimental and calculated spectra for $\alpha\text{-UO}_3$ (b), $\beta\text{-UO}_3$ (c) and $\gamma\text{-UO}_3$ (d) phases.

Up to several different U sites with variable U-Oax bond lengths are present in $\alpha\text{-UO}_3$, $\beta\text{-UO}_3$ and $\gamma\text{-UO}_3$. $\alpha\text{-UO}_3$ has two non-equivalent U positions; U forms bonds with the Oax atoms with two different average bond lengths, i.e. $\text{U}(1)\text{-Oax}_1 = 2.08$ Å and $\text{U}(2)\text{-Oax}_2 = 2.39$ Å. The uranium atoms in $\beta\text{-UO}_3$ can be divided into three groups: U(1) and U(2) have seven oxygen neighbors at distances varying between 1.69 Å and 2.72 Å, U(3) is coordinated by six oxygen atoms $\text{U}(3)\text{-Oax}_1 = 1.79$ Å, $\text{U}(3)\text{-Oax}_2 = 2.17$ Å which form a deformed octahedron, U(4) and U(5) have six oxygen neighbors and form uranyl type of bonding [17]. In $\gamma\text{-UO}_3$ all uranium atoms are surrounded by six oxygen atoms in distorted octahedral environment; the average U-Oax bond length is ≈ 1.78 Å [18]. The energy positions of features A, B and C are related to the average U-Oax distances for the three UO_3 compounds. The spectra of α - and $\gamma\text{-UO}_3$ are similar to the spectra of CaU_2O_7 and $\text{UO}_3 \cdot 1-2(\text{H}_2\text{O})$,

respectively. Therefore we propose that in average the U-Oax bonds have more covalent character in γ - UO_3 compared to α - UO_3 .

For each UO_3 phase the theoretical spectrum is a sum of weighted spectra obtained by placing the absorbing U atom at each non-equivalent crystallographic site. The FEFF9.6 code reproduces all spectral features at the correct energy positions for α - UO_3 and β - UO_3 (fig. 1 b, c); some intensity differences are present. For γ - UO_3 (fig. 1d) the distances between features A and B (A-B), and B and C (B-C) are larger for the experimental (A-B \approx 2 eV, B-C \approx 3.5 eV) compared to the calculated (A-B \approx 1.7 eV, B-C \approx 2.2 eV) spectra.

4. Conclusions

We demonstrated that a fingerprint approach using U M_4 HR-XANES can be effectively applied for characterization of "uranyl" and "uranate" type of U-Oax bonding. Using this approach we showed that U-Oax bonds have likely more covalent character in γ - UO_3 compared to α - UO_3 . The U M_4 HR-XANES spectra of the UO_3 polymorphs were performed within the full-multiple-scattering (FMS) formalism. We varied the input parameters to obtain best agreement between theory and experiment. The FEFF9.6 code emerges as a useful tool for calculation of U M_4 HR-XANES spectra, as it successfully reproduced all spectral features for some of the studied compounds.

Acknowledgements

This work is partially funded by the Russian Foundation for Basic Research (project №14-05-31488 mol_a), the joint program "Mikhail Lomonosov" of the Ministry of Education and Science of the Russian Federation and the Deutscher Akademischer Austauschdienst. We acknowledge KIT and the Helmholtz Association of German Research Centres for the Helmholtz Young Investigators Group grant (VH-NG-734) and thank ANKA for the provided beamtime. We also acknowledge Dario Manara (JRC-ITU), Xavier Gaona (INE-KIT) and Robert Baker (Trinity College Dublin) for providing part of the samples.

References

- [1] Alberman K B, Anderson J S 1949 *Angew. Chem.*, **61**, 416-416.
- [2] Hill D J 2008, *Nat. Mater.* **7**, 680.
- [3] Hoekstra HR, Siegel S J 1961 *Inorg. Nucl. Chem.*, **18**, 154-165.
- [4] Benedict M, Pigford TH, Levi HW 1981 *Nuclear Chemical Engineering, 2nd ed.*; McGraw Hill: New York.
- [5] Denecke 2006 *Coord. Chem. Rev.*, **250**, 730-754.
- [6] Bergmann U, Glatzel P 2009 *Photosynth. Res.*, **102**, 255-266.
- [7] Vitova T, Green J C, Denning R G, Loble M, Kvashnina K, Kas J J, Jorissen K, Rehr J J, Malcherek T, Denecke 2015 *Inorg. Chem.*, **54**, 174-182.
- [8] Vitova T., Denecke M A, Göttlicher J, Jorissen K, Kas J, Kvashnina K, Prüßmann T, Rehr J, Rothe J 2013 *Journal of Physics: Conference Series*, **430**, 012117.
- [9] Kvashnina K O, Butorin S M, Martin P, Glatzel P 2013 *Phys. Rev. Lett.*, **111**.
- [10] Rehr J J, Kas J J, Vila F D, Prange M P, Jorissen K 2010 *Phys. Chem. Chem. Phys.*, **12**, 5503-5513.
- [11] Gorman-Lewis D, Fein J B, Burns P C, Szymanowski J E S, Converse J 2008 *J. Chem. Thermodyn.* **40**, 980-990.
- [12] PDF-2 database, ver. 2.1402; ICDD The International Centre for Diffraction Data (www.icdd.com)
- [13] Rothe J, Butorin S, Dardenne K, Denecke M A, Kienzler B, Loble M, Metz V, Seibert A, Steppert M, Vitova T, Walther C, Geckeis H 2012 *Rev. Sci. Instrum.*, **83**.
- [14] Walshe A, Prussmann T, Vitova T, Baker R J 2014, *Dalton Trans.*, **43** (11), 4400-4407.
- [15] Rehr J J, Kas J J, Prange M P, Sorini A P, Takimoto Y, Vila F D 2009, *Comptes Rendus Physique*, **(6)**, 548-559.
- [16] Denning R G et al. 2002 *J. of Chem. Phys.*, **117**, 8008-8020.
- [17] Debets P C 1966, *Acta Cryst.*, **21**, 589.
- [18] Engmann R, de Wolff P M 1963, *Acta Cryst.*, **16**, 993.